Optimum Low-Thrust Transfer between Arbitrary Elliptic Orbits for Power-Limited Spacecraft using Asymptotic Expansions and Averaging

IEPC-2009-222

Presented at the 31st International Electric Propulsion Conference,
University of Michigan • Ann Arbor, Michigan • USA
September 20 – 24, 2009

Zahi Tarzi[1], Jason Speyer[2] and Richard Wirz[3]
UCLA, Los Angeles, CA, 90024, USA

Abstract: Low-thrust electric propulsion is increasingly being used for spacecraft missions due to its high propellant efficiency, which permits larger payloads for a given mission delta-V. As a result, trajectory optimization for low-thrust missions is becoming increasingly important. Analytical results have been obtained for limited sets of low-thrust orbit transfers, and various numerical methods have been used to obtain general solutions. However, numerical methods do not shed insight into the nature and behavior of the optimal solutions. Edelbaum obtained analytic solutions for optimum low-thrust power-limited trajectories in inverse-square force fields by utilizing the first order averaging method to obtain solutions to a limited set of elliptic transfers for the minimum fuel problem. Marec later expanded on this, refining Edelbaum's method and solving the problem for a larger set of transfers. This paper uses the same analytical methods to obtain a method of solution for the general problem of optimum transfer between two arbitrary elliptical orbits. Relations between the rates of change of the five orbital elements are obtained analytically through asymptotic expansions and averaging, and then integrated numerically to obtain the complete set of extremal paths for a given initial orbit. These paths are locally optimal until a conjugate point is reached, after which they cease to be minimizing solutions. The allowable domain of optimal paths is studied for variations in initial conditions and integration constants. A search is conducted among the paths obtained for those which meet the final boundary conditions. If a comprehensive field of trajectories has been generated, the path with the minimum payoff is globally optimal. The first order solutions obtained is valid only if many revolutions are made about the primary body.

Nomenclature

A = thrust acceleration magnitude
A_T = circumferential thrust acceleration component
A_R = radial thrust acceleration component

[1] Student, Mechanical and Aerospace Engineering, ztarzi@ucla.edu
[2] Professor, Mechanical and Aerospace Engineering, speyer@seas.ucla.edu.
[3] Assistant Professor, Mechanical and Aerospace Engineering, wirz@ucla.edu

A_W = normal thrust acceleration component
$\tilde{A}$ = defined in Eq. (118)
a = semi-major axis
$\tilde{B}$ = defined in Eq. (119)
C = constant defined in Eq. (85)
$\tilde{C}$ = defined in Eq. (120)
E = eccentric anomaly
e = eccentricity
f_{1-11} = functions defined following Eq. (7)
G = transition matrix
H = variational Hamiltonian
$H_{\lambda x}$ = defined in Eq. (121)
$\tilde{H}$ = defined in Eq. (86)
i = orbit plane inclination
J = payoff, measure of fuel consumption
k = constant defined in Eq. (90)
λ = Lagrange multiplier
M = mean anomaly
r = spacecraft trajectory radius
μ = specific gravitational constant
S = constant of integration due to spherical symmetry
t = time
Φ_{ij} = transition matrix components
φ = arc-sine of the eccentricity
Ω = longitude of the ascending node
ω = argument of periapsis

I. Introduction

With the growing use of electric propulsion systems for earth-orbiting and interplanetary spacecraft, it is becoming increasingly important to develop and understanding of the optimal trajectories for these missions. The study of optimal transfers using an electric propulsion system with variable exhaust velocity and limited power has been previously developed. The problem of rendezvous between two neighboring elliptic orbits (i.e., orbits whose orbital elements differ by a small amount) has been solved analytically by Edelbaum.[1] He then extended the treatment to include transfer between coplanar and coaxial orbits with the assumption of many revolutions required (long transfer time).[2] Marec outlined an extension of this to the general case of transfer between arbitrary elliptic orbits and analytically solved the problem for a few specific types of transfers.[3,4]

This paper utilizes the same methods as Marec and Edelbaum, but derives the problem utilizing asymptotic expansions and without transformations of the state variables. Marec's suggested method for solving the general problem is used with some alterations. A field of transfer trajectories is generated for a given initial orbit, O_0, and the optimum found for a given final orbit., O_f. In the case of rendezvous, the initial and final orbital positions (M_0, M_f) are also given. This paper does not deal with the rendezvous problem.

This problem can currently be solved using numerical methods; however, the mostly analytical treatment in this paper helps to bring to attention the variables driving the optimal paths selected. This paper uses asymptotic expansions to more fully explain the approximations which led to Edelbaum and Marec's results. Marec's proposed method of solution to the general problem is then carried out, and the nature of the optimal paths is examined through the generation of a field of trajectories for a particular initial orbit. The deformation of the surfaces which bound the domain of optimal trajectories and the points at which the trajectories cease to be locally optimizing,

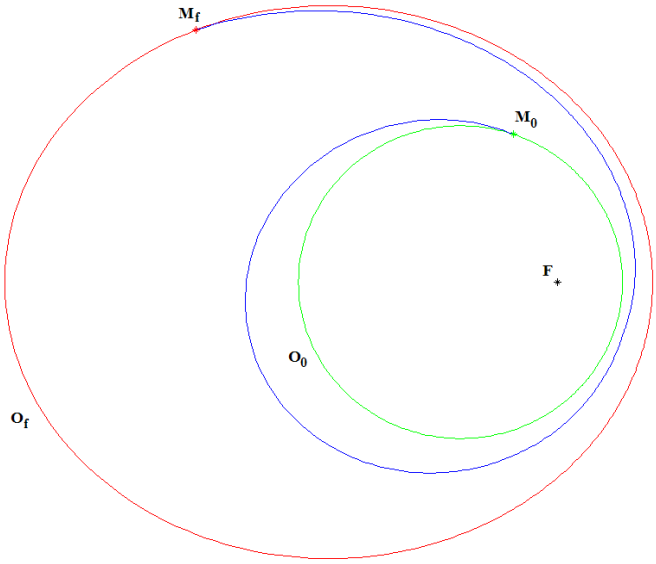

Figure 1. Elliptic Orbit Transfer

called conjugate points, are also inspected. In this way, this study sheds qualitative insight into this and similar problems involving the low-thrust optimization of spacecraft trajectories.

II.Analysis

The optimal control problem is written in the same manner as Edelbaum with the exception that the three small angles of rotation used by Edelbaum are replaced here by the argument of periapsis, inclination, and longitude of the ascending node.[1] The first order approximations made by Edelbaum are explained here by the use of asymptotic expansions. The first order differential equations for the orbital elements obtained by this method match those derived by Edelbaum.[1] From there, Marec's method of averaging the Hamiltonian is used to obtain the averaged first order differential equations.[3,4] The constants of integration are applied as proposed by Marec, but the semi-major axis is used in this paper instead of the orbital energy. Also, the constants are applied directly to the equations containing the orbital elements, instead of transforming into them afterward. This leads to the same rates of change in the orbital elements as obtained by Marec (except for the semi-major axis in place of energy).[3,4] The method of finding conjugate points used in this paper is the general method put forward by Speyer and Jacobson.[7] The solution method is similar to Marec's, but does not use a pseudo-time variable. The boundary surfaces were found as proposed by Marec, but plotted in three dimensions in order to better understand their deformations.[4] The example problem shown in this paper uses the same initial conditions as Marec, but solves the two-point boundary value problem by a searching method, whereas Marec only suggested that a search would be possible.

A. Optimization Problem

The goal is to find the trajectory which will transfer a spacecraft between two arbitrary elliptical orbits using the least amount of fuel. The optimum control problem to do this is now laid out. The six Keplerian orbital elements which fully define the motion of the spacecraft are used as the state variable. Three orthogonal components of the spacecraft thrust acceleration (circumferential, radial, and normal - A_T, A_R, A_W) are the control variables. The payoff, J, has been shown to be a measure of the fuel consumption for power-limited spacecraft and is to be minimized (-J to be maximized).[5]

$$-J = \int_{t_0}^{t_f} -\frac{A^2}{2} dt = \int_{t_0}^{t_f} -\frac{A_T^2 + A_R^2 + A_W^2}{2} dt \tag{1}$$

The state equations which completely define the motion of the spacecraft in a strong inverse-square force-field have been written previously using the Keplerian orbital elements.[1] The results are reproduced below.

$$\dot{x}_1 = da/dt = A_T f_1 + A_R f_2 \tag{2}$$

$$\dot{x}_2 = de/dt = A_T f_3 + A_R f_4 \tag{3}$$

$$\dot{x}_3 = d\omega/dt = A_T f_5 + A_R f_6 + A_W f_7 \tag{4}$$

$$\dot{x}_4 = di/dt = A_W f_8 \tag{5}$$

$$\dot{x}_5 = d\Omega/dt = A_W f_9 \tag{6}$$

$$\dot{x}_6 = dM/dt = A_T f_{10} + A_R f_{11} + \left(\mu/a^3\right)^{1/2} \tag{7}$$

where $f_i \quad i = 1,\ldots 11$ are defined in the Appendix and are function of the orbital elements and the eccentric anomaly, E. The eccentric anomaly is related to the mean anomaly, M, by Kepler's equation.

$$M = E - e\sin E \tag{8}$$

The variational Hamiltonian can now be written for this problem using Eq. (9).

$$H = -\frac{dJ}{dt} + \sum_{i=1}^{5} \lambda_i \frac{dx_i}{dt} \tag{9}$$

$$\begin{aligned} H = &-\left(A_T^2 + A_R^2 + A_W^2\right)/2 + \lambda_1\left[A_T f_1 + A_R f_2\right] + \lambda_2\left[A_T f_3 + A_R f_4\right] \\ &+ \lambda_3\left[A_T f_5 + A_R f_6 + A_W f_7\right] + \lambda_4 A_W f_8 + \lambda_5 A_W f_9 + \lambda_6\left(A_T f_{10} + A_R f_{11} + (\mu/a^3)^{1/2}\right) \end{aligned} \tag{10}$$

The Euler-Lagrange equations for the control variables are then given by Eqs. (11)-(13):

$$\partial H/\partial A_T = -A_T + \lambda_1 f_1 + \lambda_2 f_3 + \lambda_3 f_5 + \lambda_6 f_{10} = 0 \tag{11}$$

$$\partial H/\partial A_R = -A_R + \lambda_1 f_2 + \lambda_2 f_4 + \lambda_3 f_6 + \lambda_6 f_{11} = 0 \tag{12}$$

$$\partial H/\partial A_W = -A_W + \lambda_3 f_7 + \lambda_4 f_8 + \lambda_5 f_9 = 0 \tag{13}$$

Solving for the acceleration components leads to the following equations:

$$A_T = \lambda_1 f_1 + \lambda_2 f_3 + \lambda_3 f_5 + \lambda_6 f_{10} \tag{14}$$

$$A_R = \lambda_1 f_2 + \lambda_2 f_4 + \lambda_3 f_6 + \lambda_6 f_{11} \tag{15}$$

$$A_W = \lambda_3 f_7 + \lambda_4 f_8 + \lambda_5 f_9 \tag{16}$$

The rates of change of the Lagrange multipliers are given as follows.

$$\begin{aligned} d\lambda_1/dt = -\partial H/\partial a = &-\lambda_1\left[A_T\partial f_1/\partial a + A_R\partial f_2/\partial a\right] - \lambda_2\left[A_T\partial f_3/\partial a + A_R\partial f_4/\partial a\right] \\ &-\lambda_3\left[A_T\partial f_5/\partial a + A_R\partial f_6/\partial a + A_W\partial f_7/\partial a\right] - \lambda_4 A_W\partial f_8/\partial a - \lambda_5 A_W\partial f_9/\partial a \\ &-\lambda_6\left[A_T\partial f_{10}/\partial a + A_R\partial f_{11}/\partial a\right] - \lambda_6\, 3/2\left(\mu/a^5\right)^{1/2} \end{aligned} \tag{17}$$

$$\begin{aligned} d\lambda_2/dt = -\partial H/\partial e = &-\lambda_1\left[A_T\partial f_1/\partial e + A_R\partial f_2/\partial e\right] - \lambda_2\left[A_T\partial f_3/\partial e + A_R\partial f_4/\partial e\right] \\ &-\lambda_3\left[A_T\partial f_5/\partial e + A_R\partial f_6/\partial e + A_W\partial f_7/\partial e\right] - \lambda_4 A_W\partial f_8/\partial e - \lambda_5 A_W\partial f_9/\partial e \\ &-\lambda_6\left[A_T\partial f_{10}/\partial e + A_R\partial f_{11}/\partial e\right] \end{aligned} \tag{18}$$

$$d\lambda_3/dt = -\partial H/\partial\omega = -\lambda_3 A_W\partial f_7/\partial\omega - \lambda_4 A_W\partial f_8/\partial\omega - \lambda_5\partial f_9/\partial\omega \tag{19}$$

$$d\lambda_4/dt = -\partial H/\partial i = -\lambda_3 A_W\partial f_7/\partial i - \lambda_5\partial f_8/\partial i \tag{20}$$

$$d\lambda_5/dt = -\partial H/\partial\Omega = 0 \quad\Rightarrow\quad \lambda_5 = \lambda_5^0 \tag{21}$$

Where the superscript indicates initial value. The rates of change of the orbital elements can be written in terms of the Lagrange multipliers by substituting Eqs. (14)-(16) into Eqs. (2)-(7).

$$da/dt = \lambda_1\left(f_1^2 + f_2^2\right) + \lambda_2\left(f_1 f_3 + f_2 f_4\right) + \lambda_3\left(f_1 f_5 + f_2 f_6\right) + \lambda_6\left(f_1 f_{10} + f_2 f_{11}\right) \tag{22}$$

$$de/dt = \lambda_1\left(f_1 f_3 + f_2 f_4\right) + \lambda_2\left(f_3^2 + f_4^2\right) + \lambda_3\left(f_3 f_5 + f_4 f_6\right) + \lambda_6\left(f_3 f_{10} + f_4 f_{11}\right) \tag{23}$$

$$\begin{aligned} d\omega/dt = &\lambda_1\left(f_1 f_5 + f_2 f_6\right) + \lambda_2\left(f_3 f_5 + f_4 f_6\right) + \lambda_3\left(f_5^2 + f_6^2 + f_7^2\right) \\ &+\lambda_6\left(f_5 f_{10} + f_6 f_{11}\right) + \lambda_4 f_7 f_8 + \lambda_5 f_7 f_9 \end{aligned} \tag{24}$$

$$di/dt = \lambda_3 f_7 f_8 + \lambda_4 f_8^2 + \lambda_5 f_8 f_9 \tag{25}$$

$$d\Omega/dt = \lambda_3 f_7 f_9 + \lambda_4 f_8 f_9 + \lambda_5 f_9^2 \tag{26}$$

Equations (14)-(16) and (22)-(26) can be used to rewrite the Hamiltonian in terms of the Lagrange multipliers and orbital elements. In this form, it is clear that the Hamiltonian is equal to one half of the thrust acceleration magnitude squared.

$$\begin{aligned} H = \frac{1}{2}\Bigg[&\left(\lambda_1 f_1 + \lambda_2 f_3 + \lambda_3 f_5 + \lambda_6 f_{10}\right)^2 + \left(\lambda_1 f_2 + \lambda_2 f_4 + \lambda_3 f_6 + \lambda_6 f_{11}\right)^2 \\ &+\left(\lambda_3 f_7 + \lambda_4 f_8 + \lambda_5 f_9\right)^2 \Bigg] \end{aligned} \tag{27}$$

$$H = \frac{1}{2}\left[A_T^2 + A_R^2 + A_W^2\right] = \frac{1}{2}A^2 \tag{28}$$

This format is most convenient for the averaging which will be done later.

B. Asymptotic Expansion

For most low-thrust spacecraft, the thrust acceleration magnitude is very small. Thus, it is assumed that the thrust acceleration magnitude is limited by a small parameter, ε, defined as follows:

$$\varepsilon = A_{\max} << 1 \tag{29}$$

The thrust accelerations, Lagrange multipliers, and orbital elements can be asymptotically expanded based on this small parameter. The thrust acceleration is assumed to be of the same order as the small parameter based upon how it was defined.

$$A_T = (\varepsilon A_{T_0} + \varepsilon^2 A_{T_1} + \varepsilon^3 A_{T_2} + ...) \tag{30}$$

$$A_R = (\varepsilon A_{R_0} + \varepsilon^2 A_{R_1} + \varepsilon^3 A_{R_2} + ...) \tag{31}$$

$$A_W = (\varepsilon A_{W_0} + \varepsilon^2 A_{W_1} + \varepsilon^3 A_{W_2} + ...) \tag{32}$$

$$\lambda_i = (\lambda_{i_0} + \varepsilon\lambda_{i_1} + \varepsilon^2 \lambda_{i_2} + ...) \tag{33}$$

$$x_i = (x_{i_0} + \varepsilon x_{i_1} + \varepsilon^2 x_{i_2} + ...) \tag{34}$$

In this paper, subscripts will refer to asymptotic expansion order while superscripts refer to time conditions. For example, a_0 refers to the zeroth order semi-major axis whereas a^0 refers to the semi-major axis at time t = 0.

C. Zeroth Order Problem

The zeroth order problem $(\varepsilon = 0)$ is the zero thrust problem. The dynamic equations are reduced to the following:

$$\dot{a}_0 = 0 \Rightarrow \Delta a_0 = 0 \Rightarrow a_0 = a^0 \tag{35}$$

$$\dot{e}_0 = 0 \Rightarrow \Delta e_0 = 0 \Rightarrow e_0 = e^0 \tag{36}$$

$$\dot{\omega}_0 = 0 \Rightarrow \Delta \omega_0 = 0 \Rightarrow \omega_0 = \omega^0 \tag{37}$$

$$\dot{i}_0 = 0 \Rightarrow \Delta i_0 = 0 \Rightarrow i_0 = i^0 \tag{38}$$

$$\dot{\Omega}_0 = 0 \Rightarrow \Delta \Omega_0 = 0 \Rightarrow \Omega_0 = \Omega^0 \tag{39}$$

$$\dot{M}_0 = \left[\mu / a_0^3\right]^{1/2} \Rightarrow \Delta M_0 = \left[\mu / a_0^3\right]^{1/2} t \tag{40}$$

The zeroth and first order Hamiltonians are reduced to zero.

$$\left(H_0 + \varepsilon H_1 + \varepsilon^2 H_2\right) = \left(\varepsilon A_0 + \varepsilon^2 A_1 + \varepsilon^3 A_2\right)^2 \quad \Rightarrow \quad H_0 = H_1 = 0 \tag{41}$$

The equations for the thrust acceleration and Lagrange multipliers are also reduced as shown below.

$$0 = \lambda_{1_0} f_{1_0} + \lambda_{2_0} f_{3_0} + \lambda_{3_0} f_{5_0} + \lambda_{6_0} f_{10_0} \tag{42}$$

$$0 = \lambda_{1_0} f_{2_0} + \lambda_{2_0} f_{4_0} + \lambda_{3_0} f_{6_0} + \lambda_{6_0} f_{11_0} \tag{43}$$

$$0 = \lambda_{3_0} f_{7_0} + \lambda_{4_0} f_{8_0} + \lambda_{5_0} f_{9_0} \tag{44}$$

$$d\lambda_{1_0} / dt = 1.5\lambda_{6_0}^0 \left[\mu / a_0^5 \right]^{1/2} \Rightarrow \lambda_{1_0} = \lambda_{1_0}^0 + 1.5\lambda_{6_0}^0 \left[\mu / a_0^5 \right]^{1/2} t \tag{45}$$

$$d\lambda_{i_0} / dt = 0 \Rightarrow \lambda_{i_0} = \lambda_{i_0}^0 \qquad i = 2,3,4,5,6 \tag{46}$$

It is shown in the Appendix that solving Eqs. (42)-(44) lat two conditions shows that all of the Lagrange multipliers are equal to zero

D. First Order Problem

Applying the results from the zeroth order solution (all of the zeroth order Lagrange multipliers are zero) to Eqs. (17)-(21) and equating equal powers of ε leads to the following first order equations for the rates of change of the Lagrange multipliers:

$$d\lambda_{1_1} / dt = 1.5\lambda_{6_1}^0 \left[\mu / a_0^5 \right]^{1/2} \Rightarrow \lambda_{1_1} = \lambda_{1_1}^0 + 1.5\lambda_{6_1}^0 \left[\mu / a_0^5 \right]^{1/2} t \tag{47}$$

$$d\lambda_{i_1} / dt = 0 \Rightarrow \lambda_{i_1} = \lambda_{i_1}^0 \qquad i = 2,3,4,5,6 \tag{48}$$

The first order thrust accelerations can be obtained by applying the same method to Eqs. (14)-(16) and substituting Eq. (47) in for the first Lagrange multiplier .

$$A_{T_1} = \lambda_{1_0} f_{1_0} + \lambda_{2_0} f_{3_0} + \lambda_{3_0} f_{5_0} + \lambda_{6_1}^0 \left[f_{10_0} + 1.5\left(\mu / a_0 \right)^{1/2} t f_{1_0} \right] \tag{49}$$

$$A_{R_1} = \lambda_{1_0} f_{2_0} + \lambda_{2_0} f_{4_0} + \lambda_{3_0} f_{6_0} + \lambda_{6_0} f_{11_0} + \lambda_{6_1}^0 \left[f_{11_0} + 1.5\left(\mu / a_0 \right)^{1/2} t f_{2_0} \right] \tag{50}$$

$$A_{W_1} = \lambda_{3_0} f_{7_0} + \lambda_{4_0} f_{8_0} + \lambda_{5_0} f_{9_0} \tag{51}$$

These equations are equivalent to those given in Edelbaum for the optimum first order thrust acceleration programs for orbit transfer with rendezvous between neighboring orbits.[1] To solve for the transfer problem without rendezvous, the mean anomaly must be converted into a free variable. This is done by setting the Lagrange multiplier associated with it to be equal to zero. *From this point forward, this paper will only deal with optimizing the evolutions of the five remaining orbital elements.*

E. Averaging

The average of the Hamiltonian is taken by integrating it over one orbital period.

$$H = \frac{1}{2} \int_{One\,Orbit} \left[\left(\lambda_1 f_1 + \lambda_2 f_3 + \lambda_3 f_5 \right)^2 + \left(\lambda_1 f_2 + \lambda_2 f_4 + \lambda_3 f_6 \right)^2 + \left(\lambda_3 f_7 + \lambda_4 f_8 + \lambda_5 f_9 \right)^2 \right] dt \tag{52}$$

The integration variable should be changed from time to eccentric anomaly since that is the variable that this problem is periodic over. The relationship between time and eccentric anomaly can be produced by differentiating Eq. (8) with respect to time and setting it equal to Eq. (7). The resulting relationship can be used to rewrite Eq. (52) in terms of eccentric anomaly.

$$dM/dt = dE/dt\left(1-e\cos E\right) = A_T f_{10} + A_R f_{11} + \left(\mu/a^3\right)^{1/2} \tag{53}$$

$$\left[A_T f_{10} + A_R f_{11} + \left(\mu/a^3\right)^{1/2}\right] H = \frac{1}{2}\int_{E_0}^{E_0+2\pi} A^2\left(1-e\cos E\right)dE \tag{54}$$

Equation (54) is then asymptotically expanded and equal powers of ε are equated remembering that the zeroth and first order Hamiltonians are equal to zero. The result is written below in terms of the thrust acceleration in Eq. (55) and in terms of the Lagrange multipliers and orbital elements in Eq. (56).

$$H_2 = \frac{1}{2}\left(\frac{a_0^3}{\mu}\right)^{1/2}\int_{E_0}^{E_0+2\pi} A_0^2\left(1-e_0\cos E\right)dE \tag{55}$$

$$H_2 = \frac{1}{2}\left(\frac{a_0^3}{\mu}\right)^{1/2}\int_{E_0}^{E_0+2\pi}\left[\begin{array}{c}\left(\lambda_{1_1} f_{1_0} + \lambda_{2_1} f_{3_0} + \lambda_{3_1} f_{5_0}\right)^2 + \left(\lambda_1 f_{2_0} + \lambda_{2_1} f_{4_0} + \lambda_{3_1} f_{6_0}\right)^2 \\ + \left(\lambda_{3_1} f_{7_0} + \lambda_{4_1} f_{8_0} + \lambda_{5_1} f_{9_0}\right)^2\end{array}\right]\left(1-e_0\cos E\right)dE \tag{56}$$

For simplicity, the subscripts indicating asymptotic expansion order will no longer be used, but should be inferred. The averaged Hamiltonian after integration is given below.

$$\bar{H} = \frac{1}{2}\left(\frac{a}{\mu}\right)\left[\begin{array}{l}4a^2\lambda_1^2 + \frac{5}{2}\cos^2\varphi\lambda_2^2 + \left(\frac{1+5\cot^2\varphi}{2} + \frac{1+5\tan^2\varphi\sin^2\omega}{2\tan^2 i}\right)\lambda_3^2 \\ + \frac{5\tan^2\varphi\sin^2\omega}{2\sin i}\lambda_4^2 + \frac{1+5\tan^2\varphi\sin^2\omega}{2\sin^2 i}\lambda_5^2 - \frac{5\tan^2\varphi\cos\omega\sin\omega}{\tan i}\lambda_3\lambda_4 \\ - \frac{1+5\tan^2\varphi\sin^2\omega}{\tan i\sin i}\lambda_3\lambda_5 + \frac{5\tan^2\varphi\cos\omega\sin\omega}{\sin i}\lambda_4\lambda_5\end{array}\right] \tag{57}$$

Since the above equation does not contain time explicitly, the averaged Hamiltonian is a constant of the motion.

$$\bar{H} = \frac{1}{2}A^2 = \text{Constant} \tag{58}$$

The averaged state equations and rates of change of the Lagrange multipliers can be derived from the averaged Hamiltonian using Eqs. (59) and (60). This method was proposed by Marec.[3]

$$\overline{dx_i/dt} = \partial\bar{H}/\partial\lambda_i \qquad\qquad i = 1,2,3,4,5 \tag{59}$$

$$\overline{d\lambda_i / dt} = -\partial \bar{H} / \partial x_i \qquad i = 1,2,3,4,5 \tag{60}$$

The overbar indicating an average value will no longer be used in the equations for simplicity, but should be inferred. All equations after this point apply to the averaged problem. The average rates of change of the orbital elements are as follows:

$$da / dt = 4\lambda_1 \left(a^3 / \mu \right) \tag{61}$$

$$de / dt = \left(5/2 \right) \lambda_2 \left(a / \mu \right) \cos^2 \varphi \tag{62}$$

$$d\omega / dt = \left(a / \mu \right) \left[\begin{array}{l} \left(\dfrac{1 + 5\cot^2 \varphi}{2} + \dfrac{1 + 5\tan^2 \varphi \sin^2 \omega}{2 \tan^2 i} \right) \lambda_3 \\ - \dfrac{5 \tan^2 \varphi \cos\omega \sin\omega}{2 \tan i} \lambda_4 - \dfrac{1 + 5\tan^2 \varphi \sin^2 \omega}{2 \tan i \sin i} \lambda_5 \end{array} \right] \tag{63}$$

$$di / dt = \left(a / \mu \right) 5 \tan^2 \varphi \left[- \frac{\cos\omega \sin\omega}{2 \tan i} \lambda_3 \; \frac{\sin^2 \omega}{2 \sin i} \lambda_4 + \frac{\cos\omega \sin\omega}{2 \sin i} \lambda_5 \right] \tag{64}$$

$$d\Omega / dt = \left(a / \mu \right) \left[- \frac{1 + 5\tan^2 \varphi \sin^2 \omega}{2 \tan i \sin i} \lambda_3 + \frac{5 \tan^2 \varphi \cos\omega \sin\omega}{2 \sin i} \lambda_4 + \frac{1 + 5\tan^2 \varphi \sin^2 \omega}{2 \sin^2 i} \lambda_5 \right] \tag{65}$$

The average rates of change of the Lagrange multipliers are not shown here due to their complexity.

F. Constants of Integration

Due to the complex nature of the problem, the rates of change of the orbital elements cannot be solved for explicitly without the use of constants of integration which come about due to the specific nature of the problem being solved. The first of these constants has been derived previously for constant power spacecraft in a strong inverse square force-field.[5] The result is produced below along with the transformation into the Keplerian coordinate system.

$$3Ht + \vec{\lambda} \cdot \dot{\vec{r}} + 2\vec{r} \cdot \dot{\vec{\lambda}} - \vec{\lambda}^0 \cdot \dot{\vec{r}}^0 - 2\vec{r}^0 \cdot \dot{\vec{\lambda}}^0 = 5J \tag{66}$$

$$-2\lambda_1 a + 2\lambda_1^0 a_0 = 5J - 3Ht \tag{67}$$

Equation (61) can be used to obtain the first Lagrange multiplier in terms of the rate of change of the semi-major axis. This can then be used with Eq. (67) to obtain a simple differential equation for the semi-major axis.

$$\lambda_1 = \left(da / dt \right) \mu / \left(4a^3 \right) \tag{68}$$

$$\left(da / dt \right) \mu / \left(2a^2 \right) = 2\lambda_1^0 a_0 - A^2 t \tag{69}$$

This equation can be integrated to obtain the semi-major axis as a quadratic function of time. Solving this equation at the terminal condition allows for the solution of the initial Lagrange multiplier associated with the semi-major axis.

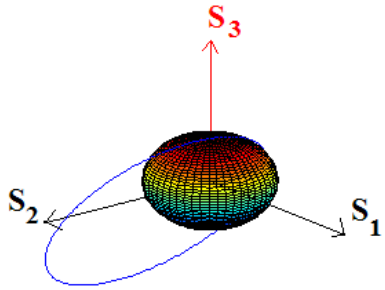

Figure 2. Vector Constant, S

$$a = \mu / \left(\mu / a_0 - 4\lambda_1^0 a_0 t + At^2 \right) \tag{70}$$

$$\lambda_1^0 = \left(At_f^2 + \mu / a_0 - \mu / a_f \right) / \left(4a_0 t_f \right) \tag{71}$$

Thus, the complete time history of the semi-major axis is known and can be solved for independently of the other orbital elements. Solving for the remaining state variables is more difficult and explicit solutions can only be obtained for special cases. However, it is possible to obtain the rates of change of the remaining orbital elements in terms of only one unknown constant. This constant of integration comes about due to the spherical symmetry of the problem. It has also been previously derived with the results shown below.[5]

$$\dot{\vec{r}} \times \vec{\lambda} + \dot{\vec{\lambda}} \times \vec{r} = \vec{S} \tag{72}$$

$$\lambda_3 = S_3 \cos i + \sin i \left(S_1 \sin \Omega - S_2 \cos \Omega \right) \tag{73}$$

$$\lambda_4 = S_2 \sin \Omega + S_1 \cos \Omega \tag{74}$$

$$\lambda_5 = S_3 \tag{75}$$

The vector constant, $\vec{S}$, is expressed in the rotating Cartesian frame shown in Fig. 2. Marec has shown that this vector constant can be selected to lie on the polar axis in order to reduce the number of scalar constants to one.[3] With this assumption, Eqs. (73)-(75) simplify to the following:

$$\lambda_3 = S \cos i \tag{76}$$

$$\lambda_4 = 0 \tag{77}$$

$$\lambda_5 = S \tag{78}$$

Applying these values to Eqs. (63)-(65) results in the following equations for the rates of change of the argument of periapsis, inclination angle, and longitude of the ascending node.

$$d\omega / dt = 5aS / \left(2\mu \right) \left(\cot^2 \varphi + \tan^2 \varphi \sin^2 \omega \right) \cos i \tag{79}$$

$$di / dt = 5aS / \left(2\mu \right) \sin i \sin \omega \cos \omega \tan^2 \varphi \tag{80}$$

$$d\Omega / dt = 5aS / \left(2\mu \right) \left(1/5 + \tan^2 \varphi \right) \sin^2 \omega \tag{81}$$

One more constant of integration must be used to solve for the rate of change of the eccentricity (in terms of the variable φ defined previously). The last equation utilized is the constant Hamiltonian, expressed below by applying Eqs. (76)-(78) to the averaged Hamiltonian from the previous section.

$$H = (a/\mu)\left[2a^2\lambda_1^2 + (5/4)\cos^2\varphi\lambda_2^2 + \left(S^2/4\right)\left(1 + 5\cot^2\varphi\cos^2 i + 5\tan^2\varphi\sin^2 i\sin^2\omega\right)\right] \quad (82)$$

Substituting for λ_1 using Eq. (67) and simplifying the results leads to Eq (83). Solving this for λ_2 and substituting into Eq. (62) results in Eq. (84).

$$5\lambda_2^2\cos^2\varphi = 5S^2\left[C - \cot^2\varphi\cos^2 i - \tan^2\varphi\sin^2 i\sin^2\omega\right] \quad (83)$$

$$\frac{d\varphi}{dt} = \pm\frac{5aS}{2\mu}\left[C - \cot^2\varphi\cos^2 i - \tan^2\varphi\sin^2 i\sin^2\omega\right]^{1/2} \quad (84)$$

where

$$C \equiv \left[2\left(2\lambda_1^0 a_0\right)^2 - 2A^2\left(\mu/a_0\right) + S^2\right]/\left(5S^2\right) \quad (85)$$

These equations for the rates of change of the five orbital elements are the same as those given by Marec.[3,4] Now the rates of change of all of the orbital elements have been obtained in terms of orbital elements and constants of integration. Numerical integration is required to carry the solution further.

G. Finding Conjugate Points

If the optimal transfer trajectory is calculated by numerical integration, it will reach a point at which it ceases to be locally optimal. This is called the conjugate point and can be found by computing the second variation of the optimal control problem. First, the variations of the rates of changed of the orbital elements and Lagrange multipliers must be found. They are given by the matrix formula below:

$$\begin{bmatrix}\delta\dot{x}\\ \delta\dot{\lambda}\end{bmatrix} = \begin{bmatrix}\tilde{A} & \tilde{B}\\ \tilde{C} & -\tilde{A}^T\end{bmatrix}\begin{bmatrix}\delta x\\ \delta\lambda\end{bmatrix} = \left[\tilde{H}\right]\begin{bmatrix}\delta x\\ \delta\lambda\end{bmatrix} \quad (86)$$

Where $\tilde{A}$, $\tilde{B}$ and $\tilde{C}$ are given as shown in the Appendix. Once they are known, the transition matrix, G, is computed as shown below.

$$\begin{bmatrix}\delta x(t_f)\\ \delta\lambda(t_f)\end{bmatrix} = \begin{bmatrix}\Phi_{11} & \Phi_{12}\\ \Phi_{21} & \Phi_{22}\end{bmatrix}\begin{bmatrix}\delta x(0)\\ \delta\lambda(0)\end{bmatrix} = G\begin{bmatrix}\delta x(0)\\ \delta\lambda(0)\end{bmatrix} \quad (87)$$

$$\left[\dot{G}\right] = \left[\tilde{H}\right][G] \quad (88)$$

This must be done numerically in concurrence with the numerical integration of the orbital elements. The conjugate point is reached when the determinate of Φ_{22} vanishes.[7] This method is used to determine when the transfer trajectory has ceased to be locally optimal.

$$\Delta(\Phi_{22}) = 0 \qquad \Rightarrow \qquad \text{Conjugate Point} \tag{89}$$

Once the conjugate point has been reached, the integration is stopped. Although this method of finding the conjugate points is not as streamlined as Marec's condensed method, it allows for better insight into the factors influencing the second variation of the optimal control problem.

Transfers between neighboring orbits should be globally optimal, transforming into locally optimal solutions as the final orbit gets further away from the initial. The point at which this transformation occurs is called a Darboux point. These points are not examined in this paper, but their investigation may be worthwhile in the future.

H. Solution Method

The method to find the trajectory which will transfer the spacecraft from one elliptic orbit to another in a specified time using the minimum amount of fuel will now be laid out. The optimal semi-major axis has already been found as a function of time. For a known thrust acceleration magnitude and transfer time, the complete time history of the semi-major axis along the optimal trajectory can be found. The rates of change of the remaining orbital elements have been expressed as functions of known variables and constants, except for one. The constant S is not known and must be guessed at in order to integrate the equations forward. A field of trajectories can be plotted for a range of S values in order to gain insight into the structure of the problem. For this purpose, working through the new constant, k, as proposed by Marec, is easier.

$$k \equiv \cot^{-1}\left(C^{1/2}\right) \tag{90}$$

Studying the rate of change of φ shed much insight into the nature of the solution. The range of k values used to generate the field of transfer trajectories is limited by it. The maximum value of k is chosen such that the initial rate of change of φ remains real. The maximum k is found by solving the below equation:

$$\left[\cot^2 k_{\min} - \cot^2 \varphi_0 \cos^2 i_0 - \tan^2 \varphi_0 \sin^2 i_0 \sin^2 \omega_0\right] = 0 \tag{91}$$

Setting the rate of change of φ equal to zero yields the surfaces which bound the domain of all possible trajectories for a given k value. The deformation of these surfaces is shown in Fig. 3 for three different k values at the initial conditions indicated below. The boundary surfaces are symmetric about both $\omega = 180°$ and $i = 180°$ and the domain of trajectories is seen to shrink as k increases (or C decreases). Given this relationship, there exists a maximum k for each initial condition to ensure that the initial rate of change of φ is real. For the initial conditions shown below, the maximum k value is slightly greater than 33°.

$$\begin{gathered}\left(a_0 = 12956km, e_0 = 0.50, \omega_0 = 210°, i_0 = 30°, \Omega_0 = 0°\right) \\ A = 5\times10^{-5} km/s^2 \qquad \mu = 3.986\times10^5 km^3/s^2 \qquad t_f = 106000s\end{gathered} \tag{92}$$

Fig 3 also shows the optimal trajectories given by these k values for the initial conditions shown. There are two possible trajectories for every k value corresponding to whether the initial rate of change of φ is assumed to be positive or negative (the consideration of negative S results in a symmetric reflection of the same trajectory field, so it is not studied here). Only the eccentricity, inclination and argument or preiapsis are studied since the semi-major axis has already been solved separately and the longitude of the ascending node can be shown to be a monotonically increasing or decreasing function of time.

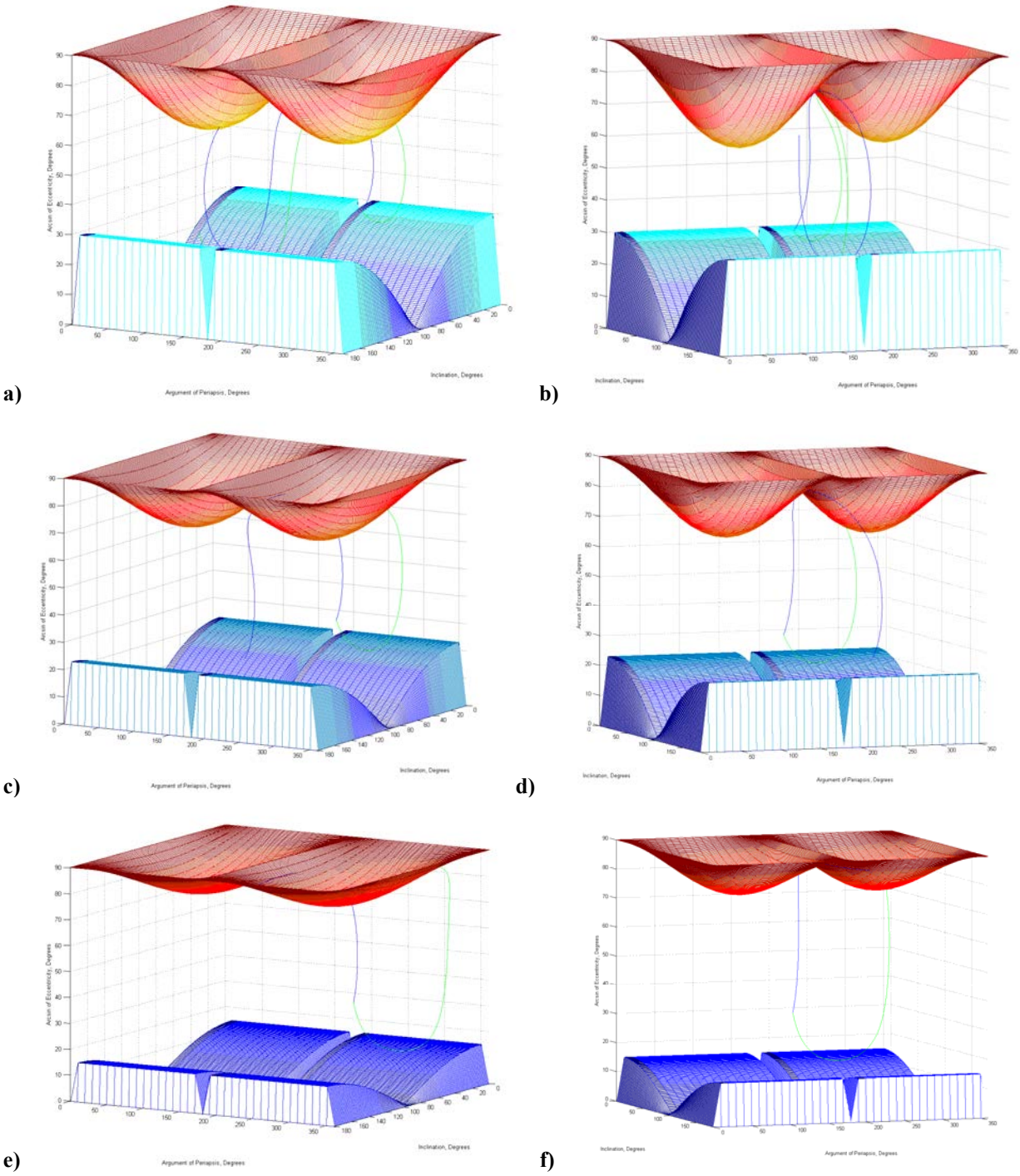

Figure 3. Boundary Surface Deformation for Small k
a,b) k = 30˚ c,d) k = 23˚ e,f) k = 15˚

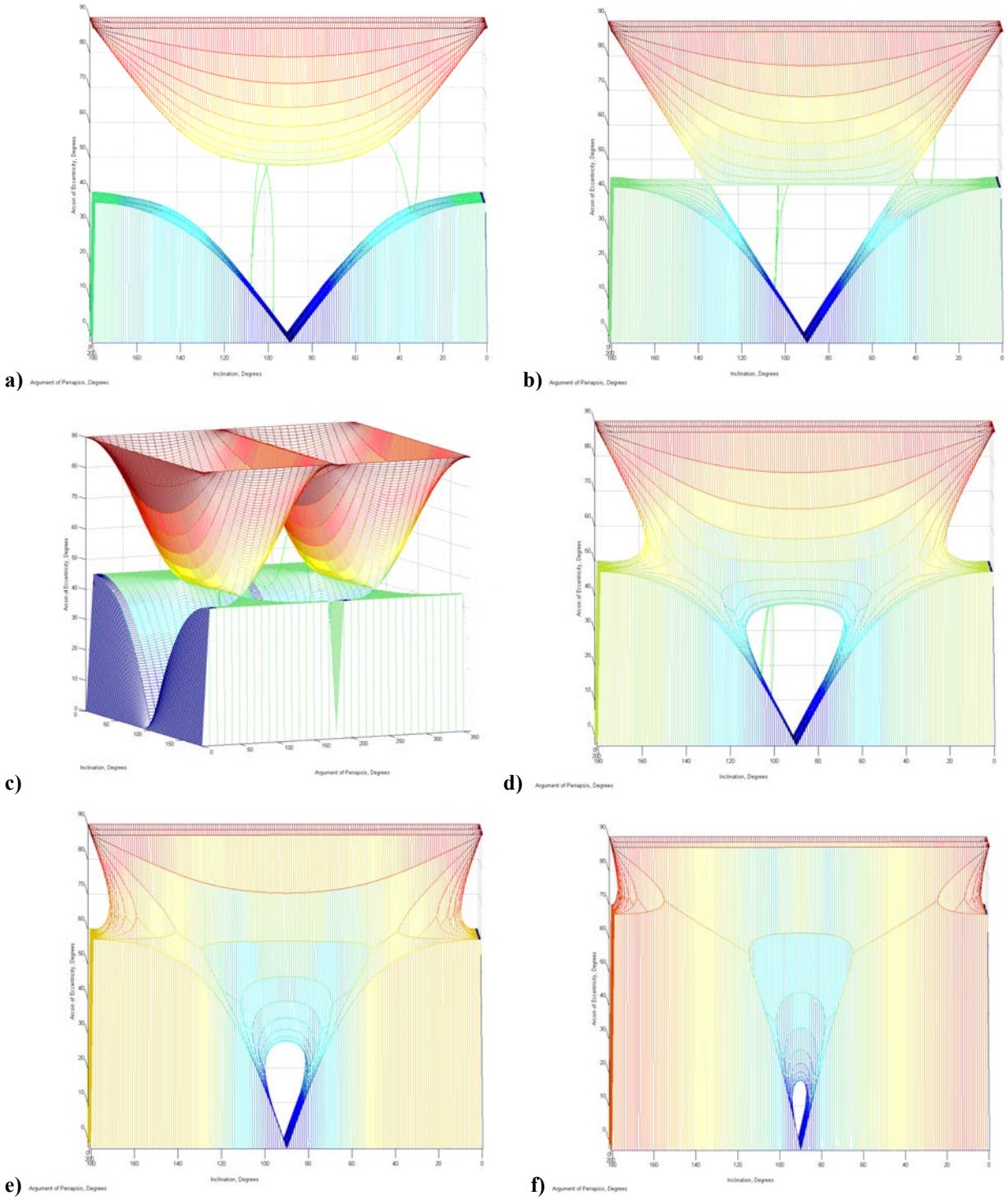

Figure 4. Boundary Surface Deformation for Large k
a) k = 40˚ b,c) k = 45˚ d) k = 50˚ e) k = 60˚ f) k = 70˚

Fig 4 shows the same boundary surface for a different set of initial conditions, those shown in Eq. **Error! Reference source not found.**. For these initial conditions, the maximum k is approximately 73˚. The plots in Fig. 4 show that when k > 45˚, the boundary surfaces grow so large that they merge together. As k increases the domain shrinks considerably, with the holes in the surfaces growing smaller for larger k values.

A field of trajectories for the same initial conditions as used in Fig. 3 is plotted in Fig. 5 for the following k values:

$$k = 13° : 33° \quad in\ steps\ of\ 1° \tag{93}$$

The conjugate points are marked at the end of each trajectory path. The minimum value of k is used in order to avoid singularities which occur in the integration for certain areas in the domain of trajectories. These problem areas are not dealt with in this paper as it is only intended to demonstrate the feasibility of such a solution and gain insight into the nature of the optimal paths.

If a comprehensive field of trajectories has been calculated, the global minimum path can be found by comparing the payoff, J, for all of the trajectories which meet the boundary conditions of the problem. In this case, a rudimentary search is conducted among the trajectories found for the one which contains the closest possible match to the desired final conditions specified below:

$$\begin{aligned} &\left(a_0 = 12956km, e_0 = 0.50, \omega_0 = 210°, i_0 = 30°, \Omega_0 = 0°\right) \\ &\left(a_f = 23598km, e_f = 0.93, \omega_f = 212.7°, i_f = 127.6°, \Omega_f = 242.5°\right) \end{aligned} \tag{94}$$

The trajectory which matches these conditions is plotted in part b of Fig. 5. In this case, the desired final orbit was known to lie within the field of optimal trajectories generated. Assuming one is able to generate a comprehensive field of trajectories, a similar method could be used to find those which result in the desired final boundary conditions. The accuracy would depend upon step size between k values and the search method used. This trajectory matches that plotted by Marec for these same initial conditions.[3,4]

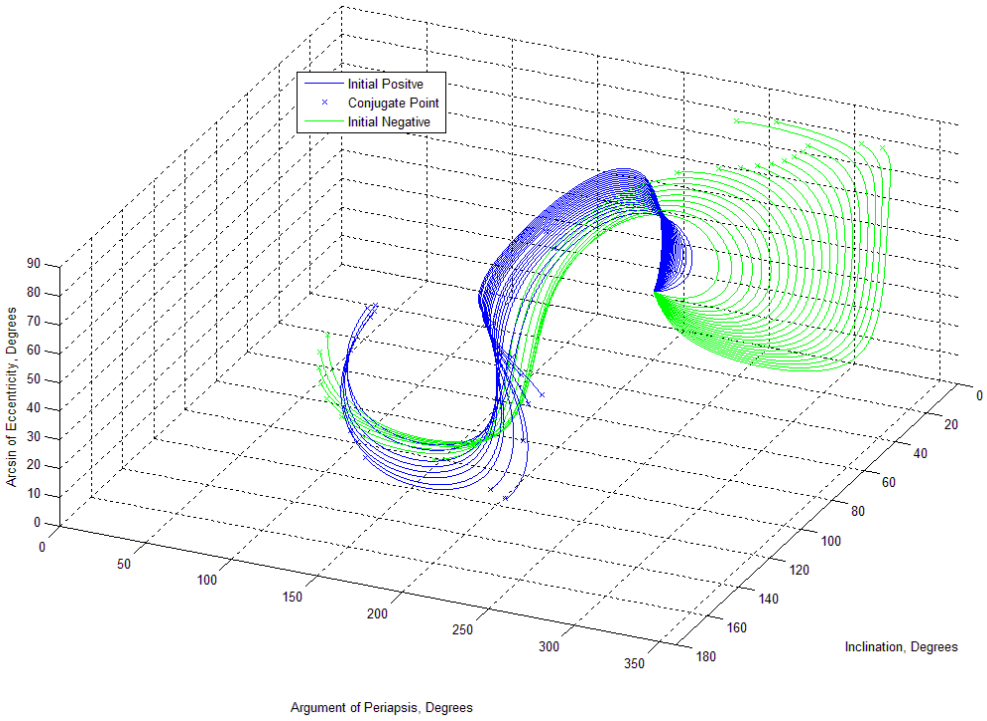

a)

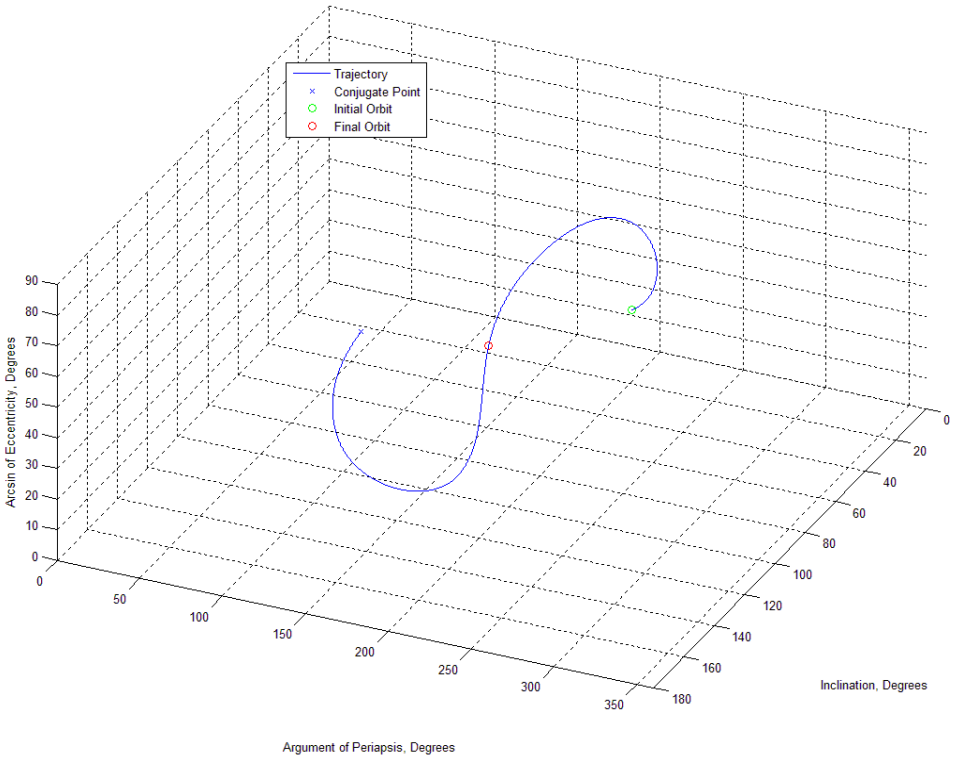

b)

Figure 5. Field of Trajectories

a) Field of optimum trajectories for initial conditions and k values indicated in text
b) Optimum trajectory corresponding to final conditions specified in text, k=30˚

Figure 6 shows the orbit evolution for the trajectory meeting the boundary conditions specified above in steps of two hundred revolutions The central body used for this demonstration is Earth. The orbit can be seen to pass through the earth at times. This is due to the fact that there are no constraints placed on the radius of the optimal trajectories.

Figure 7 shows the evolution of the orbital parameters for the trajectory which meets the boundary conditions specified above. As expected, the semi-major axis is quadratic with respect to time with the final value reached before the maximum. The eccentricity oscillates due to the change of sign that occurs when the trajectory approaches the boundary surfaces shown in Fig. 3. Then the rate of change of the eccentricity changes sign and the eccentricity decreases until the second boundary surface is reached. This continues until the conjugate point is reached. Only one sign change occurs before the final time is reached. The argument of periapsis and inclination angle pass through maxima and minima in response to the fluctuations in eccentricity. The longitude of the ascending node increases monotonically predicted earlier.

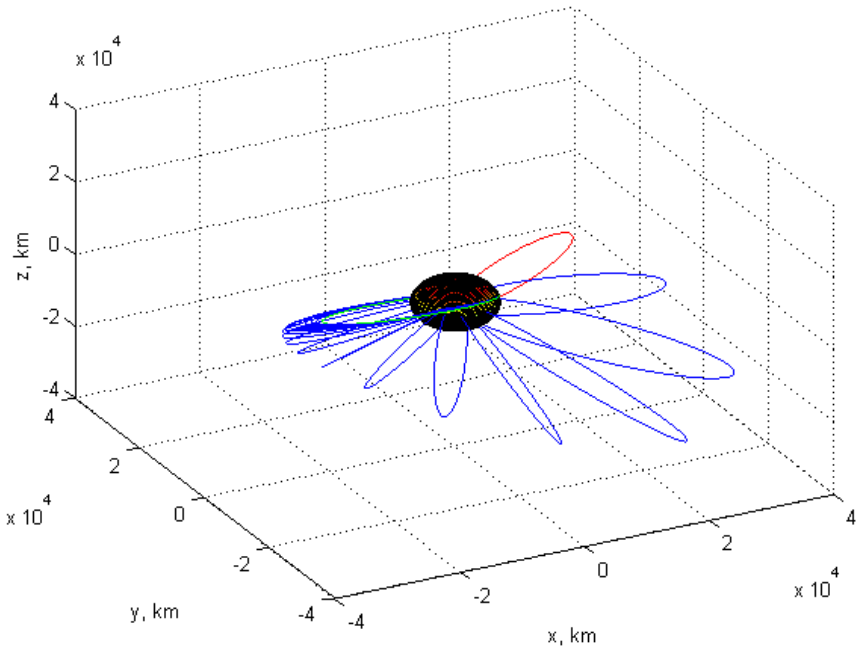

Figure 6. Elliptic Orbit Transfer

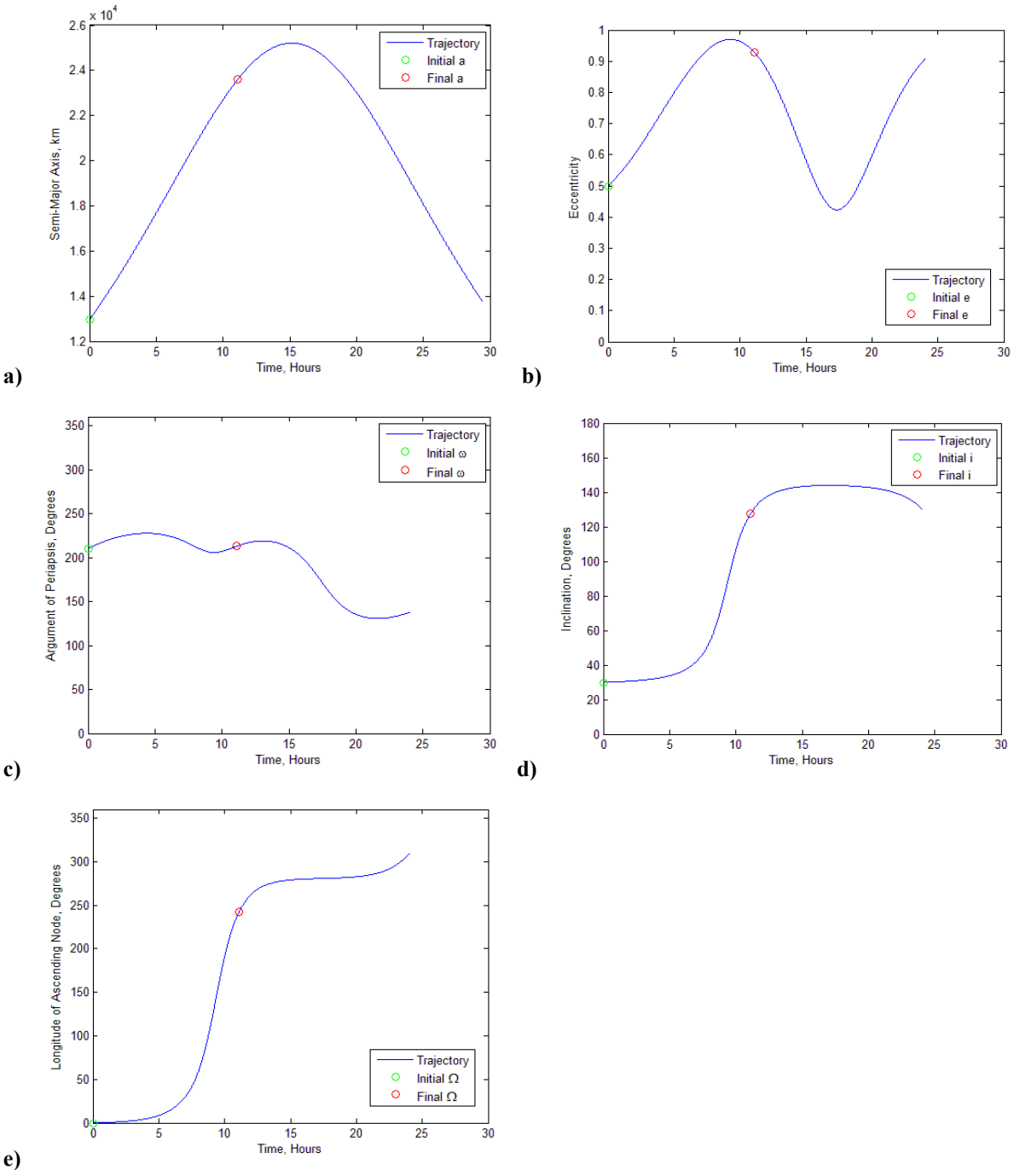

Figure 7. Evolution of Orbital Parameters
a) Semi-major axis evolution b) Eccentricity evolution c) Argument of periapsis evolutions
d) Inclination evolution e) Longitude of ascending node evolution

III. Conclusion

The study of the first order averaged problem of transfer between two elliptic orbits using a low-thrust power-limited spacecraft has been furthered by this paper. Edelbaum and Marec's solutions have been re-derived using asymptotic expansions and expanded upon to step closer to fully solving the general problem of transfer between two arbitrary elliptic orbits. Although numerical solutions presently exist which can solve this problem, the mostly analytical method presented here allows one to better understand the quality of the optimal paths which exist for these transfers and the physical parameters influencing them. The field of trajectories generated for a specific initial orbit help to envision the optimal paths possible from one point. The plots of the conjugate points and optimal trajectory boundary surfaces displayed in this paper help to clarify the forms of the of the optimal orbital element time histories. Calculation of the Darboux points would help to better understand the transformation of trajectories from globally optimal to locally optimal. Further analytical development of this method to allow trajectories to be generated and searched over the entire domain would solve the general problem and could allow for greater awareness of the nature of the optimal solution. Study of the results could aid the refinement of numerical methods and shed insight into related low-thrust optimization problems.

Appendix

A. Solution Method

The variables $f_i \quad i = 1,...11$ are defined as follows:

$$f_1 = 2\left(a^3/\mu\right)^{1/2} \frac{(1-e^2)^{1/2}}{(1-e\cos E)} \tag{95}$$

$$f_2 = 2\left(a^3/\mu\right)^{1/2} \frac{e\sin E}{\left(1-e\cos E\right)} \tag{96}$$

$$f_3 = \left(a/\mu(1-e^2)\right)^{1/2} \frac{\left(2\cos E - e\cos^2 E - e\right)}{\left(1-e\cos E\right)} \tag{97}$$

$$f_4 = \left(a/\mu\right)^{1/2} \frac{(1-e^2)\sin E}{\left(1-e\cos E\right)} \tag{98}$$

$$f_5 = \left(a/\mu\right)^{1/2} \frac{2-e\cos E - e^2}{e\left(1-e\cos E\right)} \sin E \tag{99}$$

$$f_6 = -\left(a/\mu(1-e^2)\right)^{1/2} \frac{\cos E - e}{e\left(1-e\cos E\right)} \tag{100}$$

$$f_7 = -\left(a/\mu\right)^{1/2} \frac{(1-e^2)^{1/2}\sin E\cos\omega + (\cos E - e)\sin\omega}{(1-e^2)^{1/2}\tan i} \tag{101}$$

$$f_8 = \left(a/\mu\right)^{1/2} \frac{(\cos E - e)\cos\omega - (1-e^2)^{1/2}\sin E\sin\omega}{(1-e^2)^{1/2}} \tag{102}$$

$$f_9 = \left(a/\mu\right)^{1/2} \frac{(1-e^2)^{1/2} \sin E \cos\omega + (\cos E - e)\sin\omega}{(1-e^2)^{1/2} \sin i} \tag{103}$$

$$f_{10} = -(1-e^2)^{1/2} f_5 \tag{104}$$

$$f_{11} = -(1-e^2)^{1/2} f_6 - 2\left(a/\mu\right)^{1/2} (1 - e\cos E) \tag{105}$$

B. Zeroth Order Asymptotic Solution

Equations (42)-(44) can be solved at the initial condition, E = 0. For this value of E:

$$f_{2_0}^0 = f_{4_0}^0 = f_{5_0}^0 = f_{10_0}^0 = 0 \tag{106}$$

Which leads to:

$$\left(\lambda_{1_0}^0 + 1.5\lambda_{6_0}^0 \left[\mu / a_0^5\right]^{1/2} t_0^0\right) f_{1_0}^0 = -\lambda_{2_0}^0 f_{3_0}^0 \tag{107}$$

$$\lambda_{3_0}^0 f_{3_0}^0 = -\lambda_{6_0}^0 f_{10_0}^0 \tag{108}$$

$$0 = \lambda_{3_0}^0 f_{7_0}^0 + \lambda_{4_0}^0 f_{8_0}^0 + \lambda_{5_0}^0 f_{9_0}^0 \tag{109}$$

Solving Eqs. (43) at E = π yields

$$\lambda_{3_0}^0 f_{3_0}^\pi = -\lambda_{6_0}^0 f_{10_0}^\pi \tag{110}$$

It can be shown that the third and sixth Lagrange multipliers are equal to zero by combining equations (108) and (110) and recognizing that the ratio of f_{3_0} over f_{10_0} is not the same at both time conditions.

$$f_{3_0}^0 / f_{10_0}^0 \neq f_{3_0}^\pi / f_{10_0}^\pi \quad \Rightarrow \quad \lambda_{3_0}^0 = \lambda_{6_0}^0 = 0 \tag{111}$$

Solving Eqs. (107) and (109) at E = π and using Eq. (111) to simply Eqs. (107) and (109) leads to the following four relations between the remaining Lagrange multipliers:

$$\lambda_{1_0}^0 f_{1_0}^0 = -\lambda_{2_0}^0 f_{3_0}^0 \tag{112}$$

$$\lambda_{4_0}^0 f_{8_0}^0 = -\lambda_{5_0}^0 f_{9_0}^0 \tag{113}$$

$$\lambda_{1_0}^\pi f_{1_0}^\pi = -\lambda_{2_0}^\pi f_{3_0}^\pi \tag{114}$$

$$\lambda_{4_0}^\pi f_{8_0}^\pi = -\lambda_{5_0}^\pi f_{9_0}^\pi \tag{115}$$

Using the same argument as earlier, the remaining four Lagrange multipliers can be shown to be equal to zero:

$$f_{3_0}^0 / f_{1_0}^0 \neq f_{3_0}^\pi / f_{1_0}^\pi \quad \Rightarrow \quad \lambda_{1_0}^0 = \lambda_{2_0}^0 = 0 \tag{116}$$

$$f_{8_0}^0 / f_{9_0}^0 \neq f_{8_0}^\pi / f_{9_0}^\pi \quad \Rightarrow \quad \lambda_{4_0}^0 = \lambda_{5_0}^0 = 0 \tag{117}$$

Thus, all the zeroth order Lagrange multipliers are equal to zero.

C. Finding the Conjugate Point

The matrices $\tilde{A}, \tilde{B}, \tilde{C}$ are defined as follows:

$$\tilde{A} = \begin{bmatrix} H_{\lambda_1 a} & 0 & 0 & 0 & 0 \\ H_{\lambda_2 a} & H_{\lambda_2 \varphi} & 0 & 0 & 0 \\ H_{\lambda_3 a} & H_{\lambda_3 \varphi} & H_{\lambda_3 \omega} & H_{\lambda_3 i} & 0 \\ H_{\lambda_4 a} & H_{\lambda_4 \varphi} & H_{\lambda_4 \omega} & H_{\lambda_4 i} & 0 \\ H_{\lambda_5 a} & H_{\lambda_5 \varphi} & H_{\lambda_5 \omega} & H_{\lambda_5 i} & 0 \end{bmatrix} \tag{118}$$

$$\tilde{B} = \begin{bmatrix} H_{\lambda_1 \lambda_1} & 0 & 0 & 0 & 0 \\ 0 & H_{\lambda_2 \lambda_2} & 0 & 0 & 0 \\ 0 & 0 & H_{\lambda_3 \lambda_3} & H_{\lambda_3 \lambda_4} & H_{\lambda_3 \lambda_5} \\ 0 & 0 & H_{\lambda_4 \lambda_3} & H_{\lambda_4 \lambda_4} & H_{\lambda_4 \lambda_5} \\ 0 & 0 & H_{\lambda_5 \lambda_3} & H_{\lambda_5 \lambda_4} & H_{\lambda_5 \lambda_5} \end{bmatrix} \tag{119}$$

$$\tilde{C} = \begin{bmatrix} H_{aa} & H_{a\varphi} & H_{a\omega} & H_{ai} & 0 \\ H_{\varphi a} & H_{\varphi\varphi} & H_{\varphi\omega} & H_{\varphi i} & 0 \\ H_{\omega a} & H_{\omega\varphi} & H_{\omega\omega} & H_{\omega i} & 0 \\ H_{ia} & H_{i\varphi} & H_{i\omega} & H_{ii} & 0 \\ 0 & 0 & 0 & 0 & 0 \end{bmatrix} \tag{120}$$

where

$$H_{\lambda x} = \frac{\partial H}{\partial \lambda \partial x} \tag{121}$$

The details of the above matrices are omitted due to complexity.

References

[1]Edelbaum, T.N., "Optimum Low-Thrust Rendezvous and Station Keeping," *AIAA Journal*, Vol. 2, No. 7, 1964, pp. 1196-1201.

[2]Edelbaum, T.N., "Optimum Power-Limited Orbit Transfer in Strong Gravity Fields," *AIAA Journal*, Vol. 3, No. 5, 1965, pp. 921-925.

[3]Marec, J.P., *Optimal Space Trajectories*, Elsevier Scientific Publishing Company, Amsterdam, 1979, Chaps. 6, 12.

[4]Marec, J. P., and Vinh, N.X., "General Study of Optimal Low Thrust, Limited Power Transfers Between Arbitrary Elliptical Orbits," ESA TT-697, 1981.

[5]Irving, R., "Techniques for Collision Prevention, Impact Stability, and Force Control by Space Manipulators," *Space Technology*, edited by H. S. Seifer, Progress in Astronautics and Aeronautics, AIAA, Washington, DC, 1994, pp. 175-212.

[6]Edelbaum, T.N., and Pines, S., "Fifth and Sixth Integrals for Optimum Rocket Trajectories in a Central Field," *AIAA Journal*, Vol. 8, No. 7, 1970, pp. 1201-1204.

[7]Speyer, J.L., and Jacobson, *Primer on Optimal Control Theory* , SIAM (to be published)

[8]Geffory, S, and Epenoy, R., and Noailles, J., "Averaging Technique in Optimal Control for Orbital Low-Thrust Transfers and Rendezvous Computation," *NSP Proceedings of the Twentieth International Symposium on Space Technology and Science*, Vol. 20, NSP, Gifu, Japan, 1996, pp. 449-454

[9]Bryson, A.E., and Ho, Y.C., *Applied Optimal Control*, Taylor and Francis Group, New York, 1975